Boundary cap cells are peripheral nervous system stem cells that can be redirected into central nervous system lineages

Violetta Zujovic[a,b,c,1], Julie Thibaud[a,b,c,1], Corinne Bachelin[a,b,c], Marie Vidal[a,b,c,2], Cyrille Deboux[a,b,c,2], Fanny Coulpier[d,e,f,2], Nicolas Stadler[a,b,c], Patrick Charnay[d,e,f], Piotr Topilko[d,e,f], and Anne Baron-Van Evercooren[a,b,c,g,3]

[a]Centre de Recherche de l'Institut du Cerveau et de la Moelle Epinière, Université Pierre et Marie Curie-Paris 6, Unité Mixte de Recherche (UMR) S975, 75013 Paris, France; [b]Institut National de la Santé et de la Recherche Médicale (INSERM), U975, 75013 Paris, France; [c]Centre National de la Recherche Scientifique (CNRS), UMR 7225, 75013 Paris, France; [d]INSERM, U1024, 75230 Paris, France; [e]CNRS, UMR 8197, Paris, France; [f]Ecole Normale Supérieure, 75230 Paris, France; and [g]Assistance Publique-Hôpitaux de Paris, Hôpital Pitié-Salpétrière, Fédération de Neurologie, 75230 Paris, France

Edited by Fred H. Gage, The Salk Institute, San Diego, CA, and approved April 29, 2011 (received for review December 14, 2010)

Boundary cap cells (BC), which express the transcription factor Krox20, participate in the formation of the boundary between the central nervous system and the peripheral nervous system. To study BC stemness, we developed a method to purify and amplify BC in vitro from *Krox20*$^{Cre/+}$, *R26R*$^{YFP/+}$ mouse embryos. We show that BC progeny are EGF/FGF2-responsive, form spheres, and express neural crest markers. Upon growth factor withdrawal, BC progeny gave rise to multiple neural crest and CNS lineages. Transplanted into the developing murine forebrain, they successfully survived, migrated, and integrated within the host environment. Surprisingly, BC progeny generated exclusively CNS cells, including neurons, astrocytes, and myelin-forming oligodendrocytes. In vitro experiments indicated that a sequential combination of ventralizing morphogens and glial growth factors was necessary to reprogram BC into oligodendrocytes. Thus, BC progeny are endowed with differentiation plasticity beyond the peripheral nervous system. The demonstration that CNS developmental cues can reprogram neural crest-derived stem cells into CNS derivatives suggests that BC could serve as a source of cell type-specific lineages, including oligodendrocytes, for cell-based therapies to treat CNS disorders.

dysmyelination | reprogramming | transplantation

Boundary cap cells (BC) are neural crest (NC) derivatives and were first described as discrete cell clusters localized at the dorsal root entry zone and motor exit point of the embryonic spinal cord (1). Their specific location at the central nervous system (CNS) and peripheral nervous system (PNS) interface and genetic ablation (2) showed that BC are involved in the formation of PNS–CNS boundaries. BC maintain spinal cord integrity by inhibiting motoneuron cell bodies exit to the periphery (3). Fate mapping, based on the exclusive expression of the zinc finger transcription factor Krox20 by BC between embryonic day (E)10.5 and E15.5, showed that migrating BC derivatives differentiate into Schwann cells (SC) in spinal roots, and satellite cells and a subset of nociceptive neurons in dorsal root ganglia (DRG), suggesting their multipotency (2). Hjerling-Leffler and collaborators (4) highlighted the presence of a pluripotent population in the E11 mouse DRG capable of self-renewal and differentiation into multiple NC derivatives. We reported that BC have a defined molecular signature intermediate between NC cells and SC precursors (3). Furthermore, when transplanted remotely from a focal myelin lesion of the spinal cord, BC generated remyelinating SC and few oligodendrocytes. Overall, these results strongly suggest that BC are stem cells of the embryonic PNS. However, the definition of BC stemness has been hampered by the difficulty of purifying and amplifying this restricted population. In this study, we used cell-fate mapping, FACS, and microdissection to isolate, expand, and assess BC stemness in vitro and in vivo. Our data show that BC progeny behave as stem cells that can acquire differentiation plasticity which extends beyond the PNS.

Results

BC Isolation and Expansion. Meninges were microdissected from E12.5 *Krox20*$^{Cre/+}$*: R26R*$^{YFP/+}$ mouse embryos, which allows the genetic tracing of BC derivatives (YFP$^+$) between E10.5 and E15.5 (Fig. S1 *A–C*). As previously reported, YFP$^+$ cells represent only 7 ± 1% of the total population (3), making FACS sorting difficult on a very limited number of cells. Therefore, acutely dissociated meningeal cell preparations were expanded for the short term in medium containing EGF and FGF2 (thereafter proliferation medium) (Fig. S1*D*). These conditions induced sphere formation with variable proportions of YFP$^+$ and YFP$^-$ cells (Fig. 1*A*). Spheres were next dissociated and FACS-purified (Fig. S1*E*). The percentage of YFP$^+$ cells, evaluated by immunocytochemistry prior to FACS, was not significantly different from that detected in acutely dissociated preparations (Fig. 1*C*), confirming that the ratio of YFP$^+$ and YFP$^-$ cells remained the same during the first expansion period. YFP$^+$ purified cells (thereafter YFP$^+$ cells) were further plated at semiclonal density in proliferation medium. After FACS and short-term amplification, 97 ± 3.5% of the entire population was YFP$^+$ (Fig. 1 *B* and *C* and Fig. S1*F*). Rapid expansion of the purified population showed that, like CNS (5) and NC (6, 7) -derived stem/precursor cells, BC derivatives responded successfully to EGF and FGF2 by forming spheres (Fig. 1*B*). The dynamics of YFP$^+$ cell proliferation was analyzed at 4 h after FACS and after short (passage 2; P2) and long (P9) -term culture. Combined immunocytochemistry for YFP and the cell proliferation marker Ki67 revealed that active proliferation of YFP$^+$ cells was sustained with time in culture (Fig. 1 *D–G*). To exclude the possibility that YFP$^-$ cells could give rise to YFP$^+$ cells, the FACS-sorted negative fraction was plated in proliferation medium for four passages. The absence of YFP$^+$ cells in the negative fraction indicated that the YFP$^+$ cells were exclusively derived from BC and not from cells of the negative fraction that activated Krox20 in vitro.

Specificity of BC Preparations. Stripped-off meninges could have been contaminated by central derivatives. To rule out this possibility, acutely stripped meninges on one hand and age-matched neural tube on the other were processed for RT-PCR. Data show that *Olig1* and *Olig2*, two CNS-specific transcription factors (8, 9), were detected in the neural tube but not in meningeal

Author contributions: V.Z. and A.B.-V.E. designed research; V.Z., J.T., C.B., M.V., C.D., and N.S. performed research; F.C., P.C., and P.T. contributed new reagents/analytic tools; V.Z., J.T., C.B., M.V., C.D., N.S., and A.B.-V.E. analyzed data; and V.Z., J.T., P.C., P.T., and A.B.-V.E. wrote the paper.

The authors declare no conflict of interest.

This article is a PNAS Direct Submission.

[1]V.Z. and J.T. contributed equally to this work.

[2]M.V., C.D., and F.C. contributed equally to this work.

[3]To whom correspondence should be addressed. E-mail: anne.baron@upmc.fr.

This article contains supporting information online at www.pnas.org/lookup/suppl/doi:10.1073/pnas.1018687108/-/DCSupplemental.

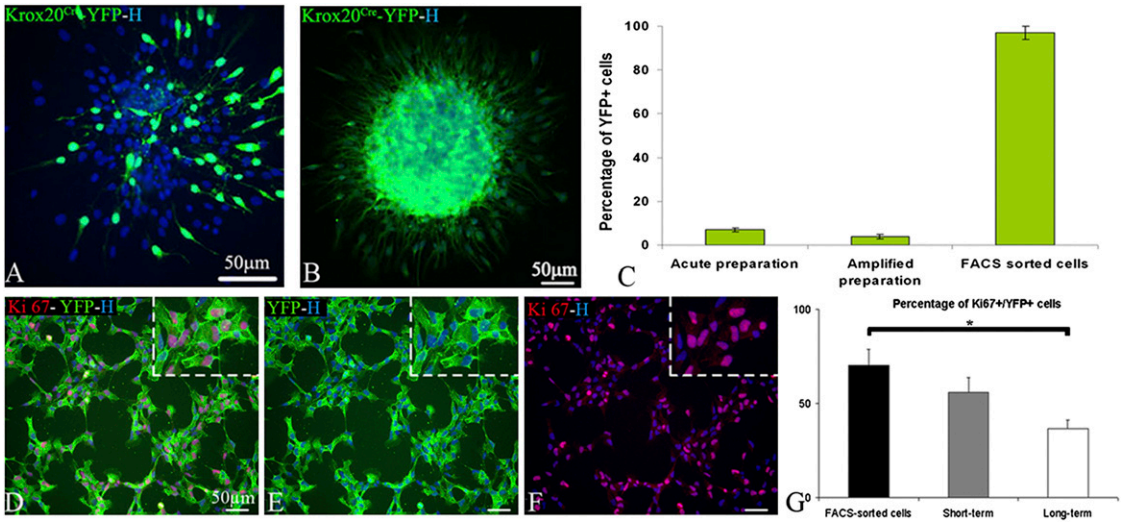

Fig. 1. Selection and amplification of YFP$^+$ cells. (*A* and *B*) Immunodetection of YFP$^+$ cells in spheres of acute cell preparations (*A*) and of FACS-sorted YFP$^+$ fraction (*B*). (*C*) Percentage of YFP$^+$ cells in acute, amplified, and FACS-sorted preparations. Combined immunocytochemistry for YFP (green; *D* and *E*) and Ki67 (red; *D* and *F*) illustrating active proliferation of FACS-purified YFP$^+$ cells. Hoechst labeling shows that the entire FACS-purified population is YFP$^+$. (*G*) Percentage of Ki67$^+$/YFP$^+$ cells at the time of FACS in short- and long-term cultures (mean ± SEM, n = 3 per group). H, Hoechst staining. (Scale bars, 50 μm.)

preparations, showing no evidence of CNS contaminants in the meningeal preparation (Fig. S2).

To exclude the possibility that BC represent a common precursor of PNS and CNS, we compared the transcriptional profiles of FACS-purified YFP$^+$ BC progeny with that of age-matched neural tube. RT-PCR analysis showed that Olig 1 transcripts were expressed exclusively in the age-matched neural tube, and NC transcripts such as *Snail* and *Slug* and BC transcripts such as *Krox20* and *L20* (2, 10) were exclusively expressed in BC progeny (Fig. S2*A*). Surprisingly, *Olig2* transcripts were expressed in both neural tube and BC derivatives. However, the absence of *Olig2* transcripts in meninges but their presence in BC derivatives indicated induction of *Olig2* transcripts upon this culture condition, as previously reported (11).

Finally, we compared the differentiation potential of neural precursor cells (NPC) and BC in the absence of EGF/FGF2 and the presence of 2% FCS (thereafter NPC differentiation medium), a condition known to induce NPC-derived oligodendrogenesis. Immunohistochemistry identified GFAP$^+$ cells in both types of cultures (Fig. S2 *D* and *G*). However, the oligodendroglial markers O4, GalC (Fig. S2 *B* and *E*), and CNPase (Fig. S2 *C* and *F*) were exclusively detected in differentiated NPC.

BC Derivative Characterization and Differentiation Potential. Our previous study indicated that BC from acutely dissociated meningeal preparations expressed the general PNS marker p75, together with immature cell markers such as Nestin, PSA-NCAM, and Sox9, but not S100β, a marker of immature and mature SC (3). Immunocharacterization of YFP$^+$ cells prior to FACS at P2 confirmed that the majority of YFP$^+$ cells expressed Nestin (94.5 ± 3%), Sox9 (86 ± 4.5%), and PSA-NCAM (85 ± 5%), whereas few cells expressed the neuronal marker β3-tubulin (7 ± 1%) or the glial fibrillary acidic protein (GFAP) (1.5 ± 1%) (Fig. 2 *A–J*), and none expressed S100β or smooth muscle antigen (SMA), a marker for myofibroblasts. Analysis of dissociated YFP$^+$ spheres after short (P4) and long (P11) -term culture showed that immature cell markers were maintained with passages whereas mature cell markers nearly vanished (Fig. 2*J*). We next performed RT-PCR analysis for multiple-lineage stage-associated transcripts on BC derivatives and adult spinal cord as control (Fig. 2*K*). NC transcripts such as *Snail* and *Slug* and BC transcripts including *Krox20* and *L20* (2, 10) were present after short- and long-term BC culture, but not in control spinal cord. Neural stem cell mRNA such as *Musashi*, *Nestin*, and *Sox9* were detected in all samples. Transcripts corresponding to more differentiated cell types such as *β3-tubulin* and *GFAP* were expressed at very low levels in BC compared with adult spinal cord. Thus, expansion of purified YFP$^+$ cells in EGF/FGF2 medium did not affect the original BC-associated transcript and protein expression pattern.

NC-related stem cells are known to give rise to multiple NC-derived lineages including neurons, glial cells, and myofibroblasts (6, 12, 13). We examined the differentiation potential of YFP$^+$ cells by culturing dissociated YFP$^+$ cells for 8 d in NC differentiation medium (6). We identified differentiated cells by immunodetection of β3-tubulin for neurons, S100β for SC, and SMA for myofibroblasts. In addition, we used GFAP in combination with p75 to discriminate astrocytes (GFAP$^+$/p75$^-$) from SC (GFAP$^+$/p75$^+$). YFP$^+$ cells demonstrated multilineage differentiation potential after short- and long-term culture with GFAP$^+$ (84.3 ± 10%) and SMA$^+$ (7.7 ± 1%) cells as major components, whereas β3-tubulin$^+$ and bipolar S100β$^+$ each constituted less than 1% of the population (Fig. 2 *L–O*). The presence of flat GFAP$^+$/p75$^-$ and β3-tubulin$^+$/p75$^-$ suggested BC spontaneous differentiation into PNS but also CNS phenotypes.

BC Migration and Differentiation Potential in the Developing *Shiverer* Brain. As a further test of BC multipotency, we grafted YFP$^+$ cells into the subventricular zone (SVZ) of the newborn *Shiverer* mouse, a dysmyelinated mutant deficient in myelin basic protein (MBP) (14). Animals were killed at postnatal day (PN) 12, 28, and 42. Immunohistochemistry at PN12 revealed extensive migration of BC-derived progeny from the graft site throughout the forebrain. YFP$^+$ cells left the SVZ and migrated into multiple brain regions including cortex, rostral migratory stream, olfactory bulb, hippocampus, corpus callosum, striatum, fimbria, thalamus, and around the fourth ventricle (Fig. S3). After the first week, many grafted cells had an immature bipolar phenotype (Fig. S3 *F–H*) characteristic of migrating cells, with orientations suggesting either a radial (corpus callosum) or a tangential (rostral migratory stream) migration mode (Fig. S4 *A* and *B*). Moreover, double immunostaining for GFAP and YFP showed that YFP$^+$ cells migrating in the rostral migratory stream were tangled within a GFAP$^+$ astrocyte network (Fig. S4 *B1–C3*), like neural precursors in the postnatal developing brain (reviewed in refs. 15–18). At later times (PN28 and PN42), YFP$^+$ cells adopted a more complex morphology as they integrated successfully into the host parenchyme (Figs. 3 and 4). Although YFP$^+$ cells proliferated

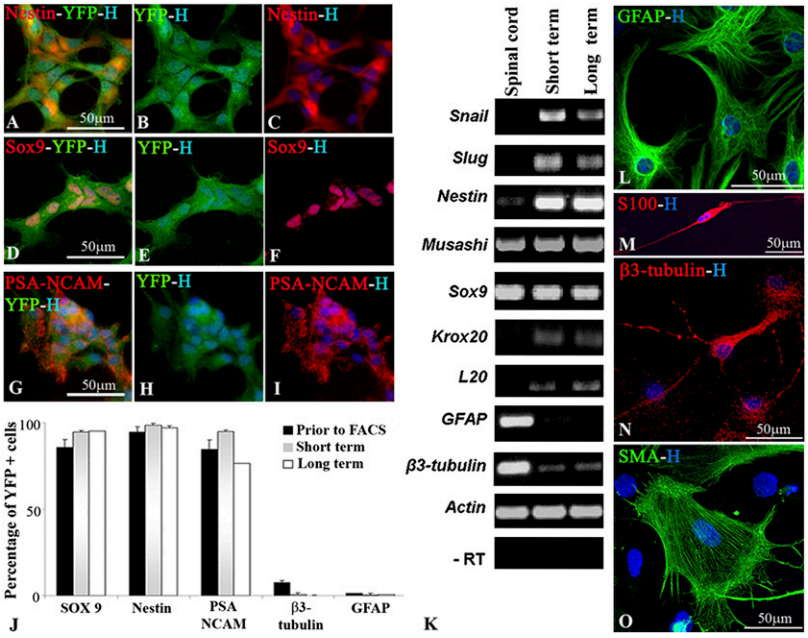

Fig. 2. Characterization and multipotency of YFP$^+$ cells in vitro. (*A–I*) Immunocharacterization of YFP$^+$ cells before FACS: YFP$^+$ cells (green) express the immature cell markers (red) Nestin (*A–C*), Sox9 (*D–F*), and PSA-NCAM (*G–I*). (*J*) Percentages of YFP$^+$ cells expressing immature cell markers are maintained after short- and long-term culture compared with YFP$^+$ cells at the time of FACS (mean ± SEM, n = 3 per group). (*K*) RT-PCR on short- and long-term FACS-sorted YFP$^+$ spheres. Total RNA from whole adult spinal cord was used as control. (*L–O*) In NC differentiation medium, YFP$^+$ cells differentiate into astrocytes (*L*), SC (*M*), neurons (*N*), and myofibroblasts (*O*).

actively in vitro, we did not observe any tumor, and grafted cells did not express Ki67 (n = 40 animals tested).

Differentiation of BC-derived cells was further assessed by immunodetection of cell type-specific antigens together with YFP. Despite their immature phenotype at PN12, very few YFP$^+$ cells expressed the immature cell markers PSA-NCAM and Sox2. In contrast, we found evidence for BC-derived progeny differentiation into GFAP$^+$ astrocytes (Fig. 3 *A–A*3), NeuN$^+$ neurons (Fig. 3 *B–B*3), and Olig2$^+$ (Fig. 3 *D*1–*D*3) or CC1$^+$ (Fig. 3 *C*1–*C*3) oligodendroglial cells. The relative proportion of each differentiated cell type varied between animals and regions. Regional analysis indicated that neuronal differentiation occurred in neurogenic regions such as thalamus (<1%) and olfactory bulb (>90%) and astrocyte differentiation occurred in cortex (>90%), thalamus (>90%), cerebellum (>90%), and meninges (>100%) and to a minor extent in corpus callosum (<10%), whereas oligodendrocyte differentiation prevailed in white-matter tracts such as corpus callosum (>90%), fimbria (>90%), and striatum but was reduced in gray matter such as cortex (<10%) (Fig. 3*E*). Some YFP$^+$ cells adopted perivascular locations. These cells expressed GFAP and extended processes to the blood vessel wall, a behavior characteristic of astrocytes involved in blood–brain barrier formation (Fig. 3 *A–A*3 and Fig. S4 *E*1–*E*3) (19–22). However, immunostaining for PECAM1 (Fig. S4*D*) or SMA to identify endothelial cells and pericytes, respectively, and careful examination by confocal microscopy excluded the possibility that the blood vessel-associated BC-derived progeny differentiated into vascular cells. We also searched for possible differentiation of grafted cells into PNS cell types. The absence of p75 expression by the grafted YFP$^+$ cells excluded this possibility and confirmed that under CNS developmental conditions, BC progeny were essentially redirected toward CNS phenotypes.

BC Derivative Differentiation into Myelin-Forming Oligodendrocytes. *shiverer* mice lacking MBP are attractive recipients for studying donor-derived myelination (23). To improve oligodendroglial cell tracking in vivo, some animals were grafted with HIV-GFP-transduced YFP$^+$ cells. The contribution of BC-derived progeny to CNS myelination was examined with antibodies against CC1 and MBP. GFP$^+$/CC1$^+$ and YFP$^+$/CC1$^+$ cells had ramified processes (Fig. 4 *A–A*3 and Fig. S5 *A*1–*A*3), and GFP$^+$/MBP$^+$ and YFP$^+$/MBP$^+$ cells showed typical features of myelin-forming cells connected to multiple processes with T-shaped endings characteristic of myelin internodes (Fig. 4 *C*1–*C*3 and Fig. S5 *B*1–*B*3). YFP labeling was excluded from compacted myelin and confined to the cell body. Moreover, YFP$^+$ and GFP$^+$ cell

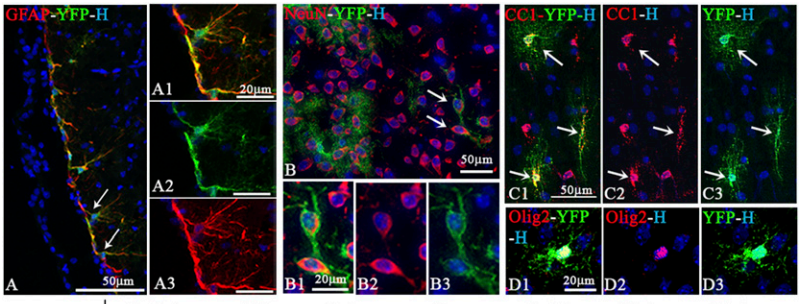

E

	Cerebellum	Cortex	Meninges	Corpus Callosum	Fimbria	Olfactory bulb	Thalamus
GFAP	>90%	>90%	100%	<10%	0	0	>90%
Neun	0	0	0	0	0	>90%	<1%
Olig2/CC1	0	<10%	0	>90%	>90%	0	0

Fig. 3. Multipotency of YFP$^+$ cells after short-term incorporation into the newborn *shiverer* brain. (*A–A3*) The majority of YFP$^+$ cells differentiate into GFAP$^+$ astrocytes, as observed in close apposition to forebrain meninges. (*B–D3*) YFP$^+$ cells differentiate in NeuN$^+$ neurons in the thalamus (*B–B3*) and in CC1$^+$ (*C1–C3*) or Olig2$^+$ (*D1–D3*) oligodendrocytes as seen in the fimbria (*C1–C3*) or corpus callosum (*D1–D3*). (*E*) Semiquantitative assessment of donor cell differentiation according to their location.

bodies were not always in the same plane as the MBP$^+$ myelin profiles, rendering quantification of donor-derived myelination difficult to achieve. Although MBP$^+$ cells or MBP$^+$ myelin was never found at P12, MBP$^+$ myelin was observed in 70% of the grafted animals at later stages (n = 20). BC-derived myelin was not restricted to the point of injection but spread in dorso-ventral and caudo-rostral directions, as MBP$^+$ structures were found in multiple brain regions including corpus callosum (Fig. 4*B*), cortex, striatum, and fimbria, as previously described for neural precursors (17, 23–25). Double immunolabeling for MBP and 2H3 to identify host neurofilaments and confocal microscopy showed *shiverer* axons clearly ensheathed by BC-derived myelin (Fig. 4*D*). Moreover, double staining for MBP and the paranodal protein Caspr showed BC-derived myelin associated with normally organized paranodes (Fig. 4 *E1*–*E3*). This suggested their contribution to the formation of nodes of Ranvier, a process that correlates with improved axonal conduction (26, 27). Because acute BC preparations grafted in the demyelinated spinal cord give rise mainly to myelin-forming SC (3), we investigated whether YFP$^+$ cells might participate in PNS myelin formation using antibodies against P0, the major peripheral myelin marker. YFP$^+$ cells and internodes expressing P0 were never detected (n = 14 animals), indicating that BC were redirected exclusively into CNS myelin-forming cells in response to CNS developmental cues. The presence of donor-derived myelin was confirmed by electron microscopy, as ultrastructural analysis of corpus callosum showed that several host axons were surrounded by compact myelin (Fig. 4 *F* and *G*). The absence of SC basement membrane and/or SC cytoplasm bordering PNS myelin confirmed that donor-derived myelin was of CNS type exclusively.

BC Differentiation into Oligodendrocytes: A Multistep Process. We next investigated in vitro the potential mechanisms involved in BC-derived oligodendrogenesis. As stated above, treatment of FACS-sorted YFP$^+$ cells with NPC differentiation medium (Fig. S2 *E*–*G*) did not induce the presence of O4-, GalC-, and CNPase-expressing cells. The emergence of oligodendrocyte precursor cells (OPC) in the embryonic neural tube and forebrain is controlled by "ventralizing" morphogens such as Noggin, an antagonizer of BMP, and Sonic hedgehog (Shh) (28). Therefore, we examined their effects on redirecting BC into OPC before their treatment with glial differentiation medium, known to promote OPC survival and/or differentiation (Table S1). Treatment with Noggin induced the generation of β3-tubulin$^+$ neurons, whereas treatment with Purmorphamine, a small molecule that activates the *Shh* pathway (29), induced the genesis of GFAP$^+$ astrocytes. When combined, these factors induced the generation of neurons and astrocytes but not oligodendrocytes.

Cells of the oligodendrocyte lineage were generated only after sequential treatment with Noggin followed by Purmorphamine (Table S1). Immunocytochemistry for oligodendroglial cell stage markers showed that BC-derived oligodendrogenesis was a multistep process (Fig. 5). Under EGF/FGF2 conditions, BC derivatives were small flat NC-like cells, expressing Olig2 (98 ± 2% of Hoechst$^+$ population) but negative for the nuclear pre-OPC transcription factor Nkx2.2 and the later oligodendroglial markers O4 and GalC (Fig. 5 *A*–*C*). After removal of EGF/FGF2 and treatment with Noggin followed by Purmorphamine, cells adopted a typical bi- or tripolar OPC-like morphology, expressing nuclear Nkx2.2 (16 ± 3% of Olig2$^+$ population) but negative for O4, GalC, or CNPase, suggesting their differentiation in pre-OPC (Fig. 5 *D*–*F*). Finally, treatment of BC-derived OPCs with glial differentiation medium induced their differentiation in multibranched oligodendrocytes with YFP$^+$ cells expressing Olig2 (Fig. S6), CNPase, O4, and GalC, indicating their ability to mature in oligodendrocytes (Fig. 5 *G*–*I*). Quantification of CNPase$^+$ cells, which outnumbered O4 and GalC$^+$ cells, indicated that they represented 5.7 ± 0.43% of the Olig2$^+$ population. RT-PCR analysis of FACS-sorted BC derivatives harvested at each step of sequential treatment confirmed the multistep differentiation process (Fig. 5*J*). Indeed, OPC transcript *PDGF receptor α* (*PDGFRα*) expression occurred in BC only after Noggin treatment, whereas mature oligodendrocyte *MBP* transcripts were detected only after Noggin/Purmorphamine pretreatment followed by glial differentiation factor media.

To prove that the mature oligodendrocytes were derived from YFP$^+$ BC progeny, we performed double labeling for YFP and CNPase and assessed that 100% of CNPase$^+$ cells were YFP$^+$ (Fig. S6).

Discussion

Using a Krox20-based Cre-lox fate-mapping approach combined with microdissection and FACS sorting, we succeeded in purifying BC discrete populations from the embryonic PNS. We demonstrate that BC are bona fide stem cells which can self-expand and differentiate into multiple lineages in vitro and in vivo. In vitro, BC progeny were EGF/FGF2-responsive and could be propagated as spheres without major modification of their immature characteristics. In NC differentiation medium, BC progeny differentiated into multiple lineages, namely myofibroblasts, glia, and neurons. BC multipotentiality was further confirmed by grafting purified BC progeny into the neonatal mouse brain. Surprisingly, the migration and differentiation patterns of grafted BC progeny were comparable with those obtained with endogenous or exogenous primary NPC in the postnatal brain (15–18). Moreover, their close association with blood vessels, suggesting their contribution to blood vessel structures or vascular tropism, was also highlighted for endogenous or transplanted NPC (19–22). Finally, BC-derived

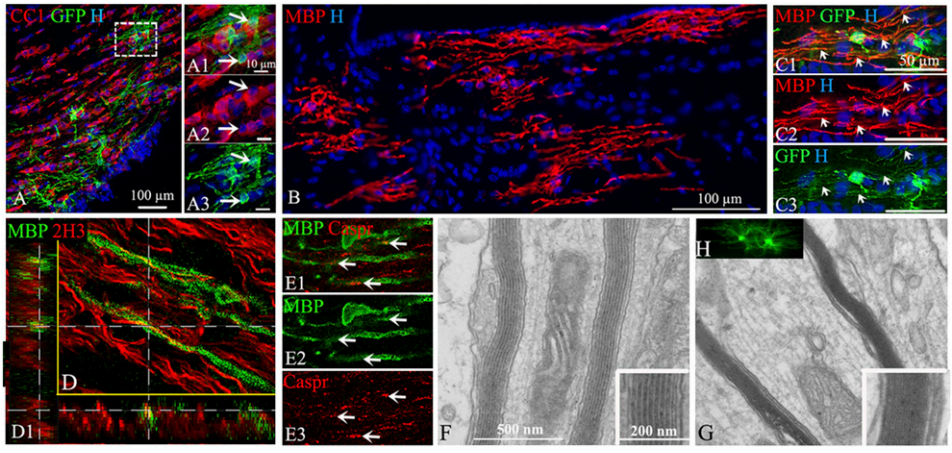

Fig. 4. Differentiation of BC progeny into myelin-forming oligodendrocytes after long-term transplantation. (*A*–*A3*) GFP$^+$ cells (green; *A* and *A2*) give rise to mature CC1$^+$ oligodendrocytes (red; *A1* and *A3*) in corpus callosum. (*B*) Immunolabeling for MBP indicates widespread BC-derived MBP$^+$ myelin patches in the fimbria. (*C1*–*C3*) Illustration of GFP$^+$ cells (green; *C1* and *C3*) expressing MBP (red; *C1* and *C2*) with features of myelin-forming oligodendrocytes extending processes to internodes (arrows). (*D* and *D1*) BC-derived MBP$^+$ myelin segments (green) surround 2H3 host axons (red); *D1* orthogonal views. (*E1*–*E3*) MBP$^+$ myelin internodes (green; *E1* and *E2*) express normally organized Caspr paranodal protein (red; *E1* and *E3*). (*F* and *G*) Ultrastructural analysis confirms the presence of compacted donor-derived myelin (*G Inset*) compared with uncompacted *shiverer* myelin (*F Inset*). (*H*) Illustration of GFP$^+$ oligodendrocytes in corresponding floating sections prior to processing for electron microscopy.

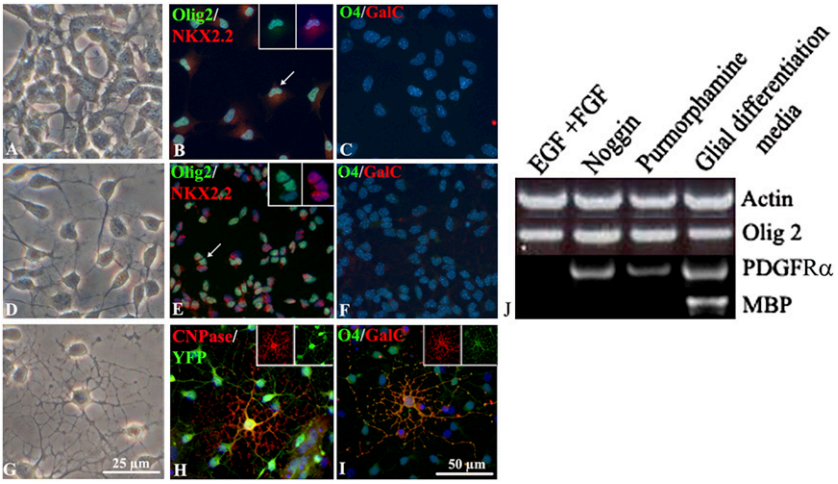

Fig. 5. In vitro BC derivative differentiation into oligodendrocytes. (*A–I*) BC progeny were grown in EGF/FGF2 medium and plated for 1 d in EGF/FGF2 alone (*A–C*), followed by sequential Noggin (3 d)/Purmorphamine (1 d) (*D–F*) or sequential Noggin (3 d)/Purmorphamine (1 d) media followed by glial differentiation medium (10 d) (*G–I*). (*A*, *D*, and *G*) Phase illustrations of morphological changes after each treatment. (*B*, *C*, *E*, *F*, *H*, and *I*) Immunocytochemistry for oligodendroglial cell stage-specific markers combined with Hoechst staining illustrating the presence of Olig2$^+$/nuclear Nkx2.2$^-$ cells (*B*) and the absence of GalC- or O4-expressing cells (*C*) in EGF/FGF2 medium, acquisition of nuclear Nkx2.2 positivity in Olig2$^+$ cells (*E*) but the absence of O4$^+$/GalC$^+$ cells (*F*) after sequential Noggin/Purmorphamine treatment, and induction of CNPase$^+$/YFP$^+$ (*H*) and O4$^+$/GalC$^+$ cells (*I*) when cells were treated with sequential Noggin/Purmorphamine media followed by glial differentiation medium. (*J*) RT-PCR on FACS-sorted BC derivatives harvested at each step of the sequential treatment. Arrows point to the magnified cells in the inset.

progeny generated the three main CNS components. The differentiation in glial cells prevailed over neuronal cells according to the temporal differentiation of these cells in situ. Moreover, BC-derived astrocytes occurred preferentially in gray matter and BC-derived oligodendrocytes in white matter (23–25). These observations indicate that BC progeny, although of NC origin, responded fully to CNS environmental cues and behaved as NPC-generating neurons, astrocytes, and oligodendrocytes without tumor formation. The glial derivatives appeared functional, as astrocytes contributed to blood vessel structures and oligodendrocytes formed myelin sheaths around axons.

Genesis of CNS derivatives was also achieved in vitro. Retrieving BC progeny from their PNS–CNS boundary location and expanding cells in EGF/FGF2 was sufficient to induce loss of PNS (p75) and acquisition of CNS (Olig2) characteristics (Fig. S2 and Fig. 4). This suggests that BC-derived cells acquired CNS features or underwent deregulation in response to EGF/FGF2 treatment as previously reported for embryonic NPC and DRG stem cells (11). However, Olig2 induction in BC progeny was not sufficient to redirect BC into cells of the oligodendrocyte lineage, as nuclear Nkx2.2 was not detected, even in conditions favoring oligodendrocyte differentiation (NPC differentiation medium). Indeed, sequential exposure to the BMP antagonizer Noggin, followed by the Shh analog Purmorphamine, was necessary to generate BC-derived pre-OPC. Finally, BC-derived OPC responded to oligodendrocyte differentiation factors, acquiring a multibranched phenotype and CNPase, O4, and GalC antigens, characteristics of mature stages of the oligodendrocyte lineage. Thus, in vitro, BC derivatives reproduce CNS developmental principles followed by differentiating embryonic stem cell-derived or primary NPC into OPC (29–32).

These in vitro observations are consistent with the fact that NC cells are responsive to BMPs, because BMPs are known to regulate NC formation and delamination (33, 34). They also highlight that antagonizing BMP signaling with Noggin in BC derivatives in vitro contributes to the loss of NC characteristics and acquisition of CNS phenotypes. Moreover, the fact that Shh was further required for the genesis of BC-derived pre-OPC correlates with its recognized role as a potent inducer of OPC in the ventral embryonic CNS (reviewed in ref. 28).

Our in vitro observations also correlate with the fact that Noggin and Shh are highly expressed in the postnatal forebrain and in particular in periventricular areas (35, 36), along with growth factors such as IGF1, PDGFA, and NT3. The availability of these environmental cues at the time of BC grafting in the newborn SVZ strongly suggests their implication in reprogramming BC progeny in oligodendrocytes in vivo. Moreover, BMPs, which are known to specify astrocytes in the postnatal brain (37), could be responsible for redirecting grafted BC in astrocytes. We show that according to their location, BC-derived progeny differentiated either in astrocytes, oligodendrocytes, or neurons. It is possible that BMPs, Noggin, and Shh act as antagonistic morphogens to promote glial diversity, and that variable expression patterns of these factors or their receptors could have favored the genesis of BC-derived astrocytes in gray matter and oligodendrocytes in white matter.

BC differentiation in CNS lineages could have resulted from the presence of CNS contaminants within the initial FACS-sorted cell preparations. However, several observations argue against this possibility. First, RT-PCR analysis of freshly harvested meninges containing BC failed to detect the CNS-specific transcription factor transcripts *Olig1* and *Olig2*, eliminating the presence of CNS contaminants in the initial preparation. Transcriptional analysis of the embryonic neural tube and BC progeny highlighted that except for *Olig2*, BC derivatives expressed transcripts clearly distinct from the neural tube, with *Slug, Snail, Krox20*, and *L20* highly specific for BC derivatives and *Olig1* highly specific for neural tube. Although *Olig2* transcripts were expressed in neural tube and BC derivatives, Olig2 positivity was not detected in situ in BC (38), confirming its in vitro induction and arguing against a possible common PNS–CNS precursor. Moreover, BC progeny acquired *PDGFRα* transcripts only when primed to differentiate into oligodendrocytes, thus demonstrating that YFP$^+$ cells were not initially contaminated by oligodendrocyte precursors but responded to CNS developmental cues to differentiate into oligodendrocytes. Second, in vitro conditions allowing differentiation of NPC into oligodendroglial cells did not suffice to induce BC-derived oligodendrogenesis. Third, in vitro induction of YFP$^+$ cells never occurred in the YFP$^-$ fraction grown in spheres, thus eliminating the possibility that YFP$^-$ contaminants became YFP$^+$. Finally, BC-derived oligodendrocytes were always YFP$^+$ both in vitro and in vivo, demonstrating unambiguously their BC origin.

In conclusion, we have developed a method for purifying BC discrete populations from the embryonic PNS and demonstrated that BC are bona fide stem cells which can self-expand and differentiate into multiple lineages in vitro and in vivo. Most importantly, our data show that CNS developmental cues can redirect PNS stem cell derivatives into CNS lineages. These appeared functional, as BC-derived astrocytes seemed to contribute to blood vessel structures, and BC-derived oligodendrocytes formed myelin around axons and participated in the formation of nodes of Ranvier. These findings obtained with a very pure and defined population of PNS stem cells substantiate BC stemness and differentiation plasticity beyond the PNS. Our findings also suggest a method for redirecting PNS stem/precursor cells into oligodendrocytes in vitro through the combined regulation of Noggin and Shh signaling. When optimized and applicable to the recently discovered NC-derived stem cells in adult DRG (6, 39) and skin (6, 40–42), this method may help the development of strategies to treat neurological disorders, including those affecting CNS myelin (43).

Materials and Methods

Animals. Mice were bred in a C57Bl6/DBA2 background. The *Krox20*$^{Cre/+}$ line contains a knock-in of the Cre recombinase-coding sequence into the *Krox20* locus (1). In *Rosa26R*$^{YFP/+}$ mice, YFP is expressed from the Rosa locus after Cre recombination (2). Recipients were 0- to 2-d-old *shiverer* mice raised in our pathogen-free animal facility. All animal protocols were performed in accordance with the guidelines of the National Institutes of Health for the Care and Use of Laboratory Animals.

Isolation of BC and NPC. Cell preparations containing BC or NPC are detailed in *SI Materials and Methods*.

Cell Culture. Amplification of cells dissociated from meninges, FACS sorting, amplification of FACS-sorted YFP$^+$ cells, cell differentiation, and cell characterization are detailed in *SI Materials and Methods*.

BC Transduction. BC transduction was performed with HIV-CMV-GFP as previously described (44) and detailed in *SI Materials and Methods*.

Cell Transplantation. Newborn mice (PN0–PN1) were cryoanesthetized and grafted with 10^5 cells from short-term amplified FACS-sorted YFP$^+$ cells (P2/P3) in 1 μL DMEM. See *SI Materials and Methods* for details.

RT-PCR Assay. RNA extraction, cDNA synthesis, and PCR were performed using standard protocols. See *SI Materials and Methods* for details.

Immunocytochemistry and Histochemistry. Immunolabelings were performed according to standard protocols for cell and tissue fixation and processing. See *SI Materials and Methods* for details.

Electron Microscopy. Tissue fixation and processing were performed according to standard protocols. See *SI Materials and Methods* for details.

ACKNOWLEDGMENTS. We thank B. Nait-Oumesmar, R. Miles, and M. Dubois-Dalcq for critically reading this manuscript; N. Sarrazin for her help in confocal microscopy, as well as E. Peles for Caspr antibody; and the Imaging and Cell sorting platforms at the Salpêtrière Hospital for technical assistance. Work in the A.B-V.E. laboratory was supported by Institute National de la Santé et de la Recherché Médicale (INSERM), National Multiple Sclerosis Society (NMSS), and Fondation de France. J.T. was supported by Aide à la Recherche sur la Sclérose en Plaque (ARSEP), NMSS, and Association Francaise contre les Myopathies (AFM). V.Z. was supported by ARSEP and NMSS. A.B.-V.E. is a recipient of a Contrat d'Interface Assistance Publique/Hopitaux de Paris (AP-HP)/Fédération de Neurologie, Hôpital Pitié-Salpêtrière. Work in the P.C. laboratory was supported by INSERM, Centre National de la Recherche Scientifique (CNRS), Ministère de la Recherche et Technologie (MRT), AFM, and Association pour la Recherche sur le Cancer (ARC).

1. Golding JP, Cohen J (1997) Border controls at the mammalian spinal cord: Late-surviving neural crest boundary cap cells at dorsal root entry sites may regulate sensory afferent ingrowth and entry zone morphogenesis. *Mol Cell Neurosci* 9:381–396.
2. Maro GS, et al. (2004) Neural crest boundary cap cells constitute a source of neuronal and glial cells of the PNS. *Nat Neurosci* 7:930–938.
3. Zujovic V, et al. (2010) Boundary cap cells are highly competitive for CNS remyelination: Fast migration and efficient differentiation in PNS and CNS myelin-forming cells. *Stem Cells* 28:470–479.
4. Hjerling-Leffler J, et al. (2005) The boundary cap: A source of neural crest stem cells that generate multiple sensory neuron subtypes. *Development* 132:2623–2632.
5. Reynolds BA, Tetzlaff W, Weiss S (1992) A multipotent EGF-responsive striatal embryonic progenitor cell produces neurons and astrocytes. *J Neurosci* 12:4565–4574.
6. Nagoshi N, et al. (2008) Ontogeny and multipotency of neural crest-derived stem cells in mouse bone marrow, dorsal root ganglia, and whisker pad. *Cell Stem Cell* 2:392–403.
7. Aquino JB, et al. (2006) In vitro and in vivo differentiation of boundary cap neural crest stem cells into mature Schwann cells. *Exp Neurol* 198:438–449.
8. Zhou Q, Anderson DJ (2002) The bHLH transcription factors OLIG2 and OLIG1 couple neuronal and glial subtype specification. *Cell* 109:61–73.
9. Lu QR, et al. (2000) Sonic hedgehog–regulated oligodendrocyte lineage genes encoding bHLH proteins in the mammalian central nervous system. *Neuron* 25:317–329.
10. Coulpier F, et al. (2009) Novel features of boundary cap cells revealed by the analysis of newly identified molecular markers. *Glia* 57:1450–1457.
11. Dromard C, et al. (2007) NG2 and Olig2 expression provides evidence for phenotypic deregulation of cultured central nervous system and peripheral nervous system neural precursor cells. *Stem Cells* 25:340–353.
12. Morrison SJ, White PM, Zock C, Anderson DJ (1999) Prospective identification, isolation by flow cytometry, and in vivo self-renewal of multipotent mammalian neural crest stem cells. *Cell* 96:737–749.
13. Shah NM, Groves AK, Anderson DJ (1996) Alternative neural crest cell fates are instructively promoted by TGFβ superfamily members. *Cell* 85:331–343.
14. Mikoshiba K, et al. (1982) Oligodendrocyte abnormalities in shiverer mouse mutant are determined in primary chimaeras. *Nature* 299:357–359.
15. Baulac M, et al. (1987) Transplantation of oligodendrocytes in the newborn mouse brain: Extension of myelination by transplanted cells. Anatomical study. *Brain Res* 420:39–47.
16. Suzuki SO, Goldman JE (2003) Multiple cell populations in the early postnatal subventricular zone take distinct migratory pathways: A dynamic study of glial and neuronal progenitor migration. *J Neurosci* 23:4240–4250.
17. Vitry S, Avellana-Adalid V, Lachapelle F, Evercooren AB (2001) Migration and multipotentiality of PSA-NCAM$^+$ neural precursors transplanted in the developing brain. *Mol Cell Neurosci* 17:983–1000.
18. Brazel CY, Romanko MJ, Rothstein RP, Levison SW (2003) Roles of the mammalian subventricular zone in brain development. *Prog Neurobiol* 69:49–69.
19. Louissaint A, Jr., Rao S, Leventhal C, Goldman SA (2002) Coordinated interaction of neurogenesis and angiogenesis in the adult songbird brain. *Neuron* 34:945–960.
20. Palmer TD, Willhoite AR, Gage FH (2000) Vascular niche for adult hippocampal neurogenesis. *J Comp Neurol* 425:479–494.
21. Pluchino S, Martino G (2008) Neural stem cell-mediated immunomodulation: Repairing the haemorrhagic brain. *Brain* 131:604–605.
22. Tavazoie M, et al. (2008) A specialized vascular niche for adult neural stem cells. *Cell Stem Cell* 3:279–288.
23. Lachapelle F, et al. (1983-1984) Transplantation of CNS fragments into the brain of shiverer mutant mice: Extensive myelination by implanted oligodendrocytes. I. Immunohistochemical studies. *Dev Neurosci* 6:325–334.
24. Levison SW, Chuang C, Abramson BJ, Goldman JE (1993) The migrational patterns and developmental fates of glial precursors in the rat subventricular zone are temporally regulated. *Development* 119:611–622.
25. Yandava BD, Billinghurst LL, Snyder EY (1999) "Global" cell replacement is feasible via neural stem cell transplantation: Evidence from the dysmyelinated shiverer mouse brain. *Proc Natl Acad Sci USA* 96:7029–7034.
26. Black JA, Waxman SG, Smith KJ (2006) Remyelination of dorsal column axons by endogenous Schwann cells restores the normal pattern of Nav1.6 and Kv1.2 at nodes of Ranvier. *Brain* 129:1319–1329.
27. Sasaki M, et al. (2001) Transplantation of an acutely isolated bone marrow fraction repairs demyelinated adult rat spinal cord axons. *Glia* 35:26–34.
28. Guillemot F (2007) Cell fate specification in the mammalian telencephalon. *Prog Neurobiol* 83:37–52.
29. Hu BY, Du ZW, Zhang SC (2009) Differentiation of human oligodendrocytes from pluripotent stem cells. *Nat Protoc* 4:1614–1622.
30. Samanta J, Kessler JA (2004) Interactions between ID and OLIG proteins mediate the inhibitory effects of BMP4 on oligodendroglial differentiation. *Development* 131:4131–4142.
31. Zhang SC, Lundberg C, Lipsitz D, O'Connor LT, Duncan ID (1998) Generation of oligodendroglial progenitors from neural stem cells. *J Neurocytol* 27:475–489.
32. Lavdas AA, Franceschini I, Dubois-Dalcq M, Matsas R (2006) Schwann cells genetically engineered to express PSA show enhanced migratory potential without impairment of their myelinating ability in vitro. *Glia* 53:868–878.
33. Du ZW, Li XJ, Nguyen GD, Zhang SC (2006) Induced expression of Olig2 is sufficient for oligodendrocyte specification but not for motoneuron specification and astrocyte repression. *Mol Cell Neurosci* 33:371–380.
34. Sela-Donenfeld D, Kalcheim C (1999) Regulation of the onset of neural crest migration by coordinated activity of BMP4 and Noggin in the dorsal neural tube. *Development* 126:4749–4762.
35. Lim DA, et al. (2000) Noggin antagonizes BMP signaling to create a niche for adult neurogenesis. *Neuron* 28:713–726.
36. Palma V, et al. (2005) Sonic hedgehog controls stem cell behavior in the postnatal and adult brain. *Development* 132:335–344.
37. Zhang D, Mehler MF, Song Q, Kessler JA (1998) Development of bone morphogenetic protein receptors in the nervous system and possible roles in regulating trkC expression. *J Neurosci* 18:3314–3326.
38. Coulpier F, et al. (2010) CNS/PNS boundary transgression by central glia in the absence of Schwann cells or Krox20/Egr2 function. *J Neurosci* 30:5958–5967.
39. Li HY, Say EH, Zhou XF (2007) Isolation and characterization of neural crest progenitors from adult dorsal root ganglia. *Stem Cells* 25:2053–2065.
40. Biernaskie J, et al. (2009) SKPs derive from hair follicle precursors and exhibit properties of adult dermal stem cells. *Cell Stem Cell* 5:610–623.
41. Hunt DP, et al. (2008) Effects of direct transplantation of multipotent mesenchymal stromal/stem cells into the demyelinated spinal cord. *Cell Transplant* 17:865–873.
42. Hunt DP, et al. (2010) Origins of gliogenic stem cell populations within adult skin and bone marrow. *Stem Cells Dev* 19:1055–1065.
43. Martino G, Franklin RJ, Baron Van Evercooren A, Kerr DA; Stem Cells in Multiple Sclerosis (STEMS) Consensus Group (2010) Stem cell transplantation in multiple sclerosis: Current status and future prospects. *Nat Rev Neurol* 6:247–255.
44. Bachelin C, Zujovic V, Buchet D, Mallet J, Baron-Van Evercooren A (2010) Ectopic expression of polysialylated neural cell adhesion molecule in adult macaque Schwann cells promotes their migration and remyelination potential in the central nervous system. *Brain* 133:406–420.